INSTITUT DE FRANCE
Académie des sciences

Comptes Rendus

Physique

Frédéric Caupin

Fluid inclusions in minerals: from geosciences to the physics of water and back

Volume 23, Special Issue S2 (2022), p. 71-87

Published online: 19 December 2022
Issue date: 19 June 2023

https://doi.org/10.5802/crphys.127

Part of Special Issue: Prizes of the French Academy of Sciences 2021

Les Comptes Rendus. Physique *sont membres du*
Centre Mersenne pour l'édition scientifique ouverte
www.centre-mersenne.org
e-ISSN : 1878-1535

Comptes Rendus
Physique
2022, Vol. 23, Special Issue S2, p. 71-87
https://doi.org/10.5802/crphys.127

Prizes of the French Academy of Sciences 2021 / *Prix 2021 de l'Académie des sciences*

Fluid inclusions in minerals: from geosciences to the physics of water and back

Inclusions fluides dans les minéraux : un aller-retour entre géosciences et physique de l'eau

Frédéric Caupin *, [a]

[a] Institut Lumière Matière, Université de Lyon, Université Claude Bernard Lyon 1, CNRS, Institut universitaire de France, F-69622, Villeurbanne, France
E-mail: frederic.caupin@univ-lyon1.fr (F. Caupin)

Abstract. Natural mineral samples often contain small volumes of trapped fluid material. They carry information about the history of the host mineral and its environment, and for this reason are used by geoscientists. Physicists and physico-chemists have successfully harnessed water inclusions in quartz to bring liquid water to a metastable state, at a pressure well below its equilibrium pressure with vapor. The pressure can reach negative values as large as −140 MPa, which exceeds by far the limits of other techniques, and approaches the theoretical threshold for spontaneous nucleation of a vapor bubble. This has enabled a deeper understanding of nucleation and of the anomalies of water. In turn, the optical techniques developed to study water's properties have recently found a new application in the reconstruction of palaeotemperatures in surface processes. I review here some aspects of fluid inclusions, these fascinating objects at the crossroads between disciplines.

Résumé. Les échantillons de minéraux naturels contiennent souvent de petits volumes de matière fluide piégée. Ils transmettent des informations sur l'histoire du minéral hôte et de son environnement, ce qui leur vaut d'être utilisés par les géologues. Les physiciens et physico-chimistes ont réussi à exploiter les inclusions d'eau dans le quartz pour porter l'eau liquide dans un état métastable, à une pression bien inférieure à sa pression d'équilibre avec la vapeur. La pression peut atteindre des valeurs négatives aussi élevées que −140 MPa, ce qui dépasse de loin les limites des autres techniques et s'approche du seuil théorique de nucléation spontanée d'une bulle de vapeur. Cela a permis de mieux comprendre la nucléation et les anomalies de l'eau. À leur tour, les techniques optiques développées pour étudier les propriétés de l'eau ont récemment trouvé une nouvelle application dans la reconstruction des paléotempératures des processus de surface. Je passe ici en revue quelques aspects des inclusions fluides, objets fascinants au carrefour des disciplines.

Keywords. Water, Metastability, Nucleation, Thermodynamic anomalies, Palaeotemperatures, Interdisciplinarity.

Mots-clés. Eau, Métastabilité, Nucléation, Anomalies thermodynamiques, Paléotempératures, Interdisciplinarité.

Funding. The author is supported by Agence Nationale de la Recherche, grant number ANR-19-CE30-0035-1.

* Corresponding author.

Note. Frédéric Caupin is the 2021 recipient of the Cécile Dewitt-Morette / École de Physique des Houches Prize.

Published online: 19 December 2022, Issue date: 19 June 2023

1. Introduction

Pluridisciplinary approaches have long been recognized as fruitful ways to perform research. The purpose of this article is to tell a story about how the fields of geosciences and physics have experienced cross-fertilization, thanks to a tiny, but powerful, tool: fluid inclusions in minerals. I will first introduce the topic of negative pressure in water (Section 2), which is an example of metastability: *liquid* water can be observed at temperature and pressure conditions at which it is not the most stable state. Section 3 presents fluid inclusions in minerals, well known to geoscientists, and Section 4 explains how physicists and physico-chemists have brought them into their field for studying the properties of metastable water. Finally, in Section 5, I will present our recent trip back to geosciences, bringing along a new thermometer to constrain past temperatures.

Before starting our journey, a disclaimer: I am not a geoscientist. I benefit from the collaboration with colleagues in geosciences. I apologize in advance for the very basic survey I will give of geological topics. I invite the reader to consult the cited reviews for more authoritative accounts.

2. Negative pressure in water

I give here a brief introduction to the topic of water at negative pressure.

2.1. *What is negative pressure?*

When I talk about negative pressure in a liquid, I often get the following question: "Pressure cannot be negative, so you're talking about *relative* pressure, right?" Pressure *in a gas* cannot be negative indeed, because the gas atoms or molecules are so far apart that they cannot resist mechanical tension. But the molecules in a liquid or in a solid are much closer. Their mutual attraction is responsible for the cohesion of these materials. This appears natural when talking about a solid: one can pull on both ends of a stick quite hard before it breaks. The situation, although less common, is similar in a liquid. So, no, I am not talking about relative pressure, but about *absolute* negative pressure, when the liquid experiences mechanical tension. This statement becomes much less shocking when thinking in terms of density. Density of water at ambient pressure and temperature is around $1000\,\mathrm{kg\,m^{-3}}$. When the pressure goes negative, the density simply decreases, by as much as 9 % (see Section 4.2), which corresponds to an average distance between molecules increased by around 3 %.

In fact, you may walk close to negative pressures everyday without knowing it. Trees indeed use negative pressure to pull the sap up their trunks. The ascending sap (nearly pure water) forms a continuous liquid column from the roots to the leaves. Hydrostatics teaches us that the pressure in water decreases by 0.1 MPa for every 10 m ascent, so that the sap pressure is indeed negative in tall trees! Of course, the details are more complicated, and other parameters (drought, vessel diameter, etc…) must be taken into account, see Refs. [1, 2] for reviews.

Similar to a rod, there is a limit to the mechanical tension in a liquid, which is called the tensile strength. However, in a liquid, the failure mechanism is different: a vapor bubble appears, rather than a crack. The simplest theory for the tensile strength of a liquid is presented in the next Section.

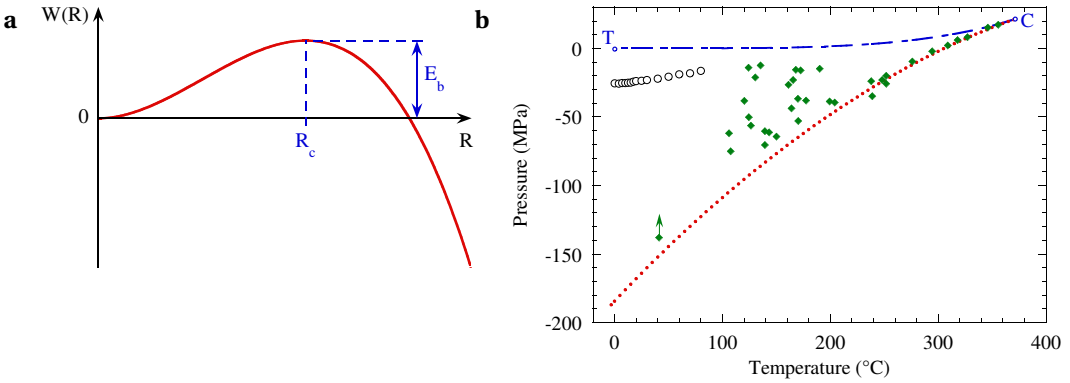

Figure 1. a) Work $W(R)$ required to form a bubble in a liquid at negative pressure as a function of its radius R; the maximum E_b is reached at the critical radius R_c. **b)** Cavitation pressure in water as a function of temperature. The dash-dotted blue curve shows the equilibrium vapor pressure from the triple point T to the critical point C. The dotted red curve is the prediction from classical nucleation theory. The symbols show the experimental values for acoustic cavitation (empty black circles) [3] and for fluid inclusions in quartz (filled green diamonds) [4]. Adapted from Ref. [5].

2.2. *Classical nucleation theory*

I will give here only a brief summary of the results of classical nucleation theory, and refer the reader to Refs. [5–8] for detailed accounts. Consider a liquid at temperature T and at large negative pressure P below the saturated vapor pressure $P_\mathrm{sat}(T)$. Neglecting $P_\mathrm{sat}(T) \ll -P$, the minimum work required to create a vapor bubble of radius R is:

$$W(R) = \frac{4}{3}\pi R^3 P + 4\pi R^2 \sigma \tag{1}$$

where σ is the liquid-vapor surface tension. The first term is an energy gain corresponding to the replacement of a volume of liquid by a more stable vapor phase, and the second term is an energy cost associated with the creation of a liquid-vapor interface. $W(R)$, displayed in Figure 1 a, shows a maximum at the critical radius $R_\mathrm{c} = 2\sigma/R$, defining the energy barrier:

$$E_\mathrm{b} = \frac{16\pi}{3}\frac{\sigma^3}{P^2}. \tag{2}$$

This explains why the liquid can remain metastable: bubbles with radius less than R_c will disappear. If the bubble radius exceeds R_c, it will then grow spontaneously, terminating the metastability of the liquid. This process, known as nucleation, is typical of first-order phase transitions, because of the existence of a surface tension σ. In the present case of liquid to vapor nucleation, it is also called cavitation. Cavitation will occur during an observable time when E_b becomes of the order of a few tens of the available thermal energy $k_\mathrm{B}T$, where k_B is Boltzmann's constant. Figure 1 b shows the cavitation pressure predicted for water [5], around $P = -150\,\mathrm{MPa}$ at room temperature. This extreme negative pressure results from the large surface tension of water, due to its hydrogen bonds which make it a highly cohesive liquid. Also shown in Figure 1 b are two sets of experimental data discussed in the next section.

2.3. *Tensile strength of water*

I have written an in-depth review of cavitation in water in this journal [5]. I will not repeat it here, but I cannot resist mentioning who first observed cavitation in water at negative pressure:

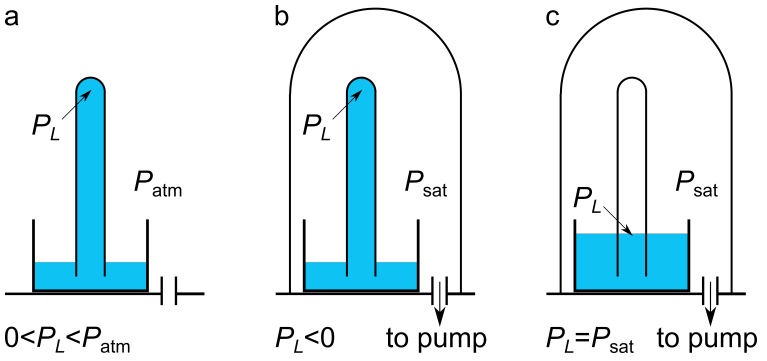

Figure 2. A sketch of Huygens' experiment [9–11]. A Torricellian experiment is prepared: a tube open at one end is filled with water, and the open end immersed in water in a container. Water remains in the tube because of the atmospheric pressure outside (**a**). After evacuating the surrounding air with a pump, the water level in the tube remains unchanged (**b**), so that water at the top is stretched. If a bubble enters the tube from its lower end, it moves upwards, expands, and the water level drops (**c**).

Christiaan Huygens. Among the very first members of the French Academy of Sciences (funded in 1666), Huygens performed his experiment in December 1661; see Ref. [9] for the original article in French, Ref. [10] for a partial English translation, and Ref. [11] for the fascinating full story. Huygens' experiment is sketched in Figure 2. A tall tube open at one end is filled with water and placed vertically with its mouth in a low-profile container, also filled with water (Figure 2 a); the atmospheric pressure prevents the liquid from falling. The setup is placed in a vacuum pump. When air is evacuated, one would expect the water level in the tube to drop to the same height as the water in the outer container. Yet, to Huygens' surprise, the level in the tube remained unchanged (Figure 2 b). From hydrostatics, liquid water at the top is thus at a pressure lower than the saturated vapor pressure, and even negative for a long enough tube. Only when a bubble is placed at the lower end of the tube, it moves upwards and suddenly expands to nearly occupy the full length of the tube, making the water drop (Figure 2 c).

Many experiments, described in Refs. [5, 12], were performed since. For instance, negative pressures were generated by cooling water at constant volume (see also Section 4.1), or using the centrifugal force when spinning a tube, or focusing an acoustic wave. Our results with the latter technique [3, 13, 14] are displayed in Figure 1 b. All these experiments obtained cavitation pressures near −30 MPa at room temperature.

At room temperature, there is therefore a large discrepancy between the threshold observed by different techniques ($\simeq -30$ MPa), and the theoretical prediction ($\simeq -150$ MPa, see Section 2.2). We shall see that fluid inclusions in minerals, present in Nature (see Section 3.1), have been used to mend this gap and bring water to the theoretical limit (Section 4).

3. Fluid inclusions in minerals

This section gives a brief introduction to fluid inclusions (Section 3.1) and some of their notable uses in Geosciences (Section 3.2). For much more details, the reader is referred to specialized reviews [15–17].

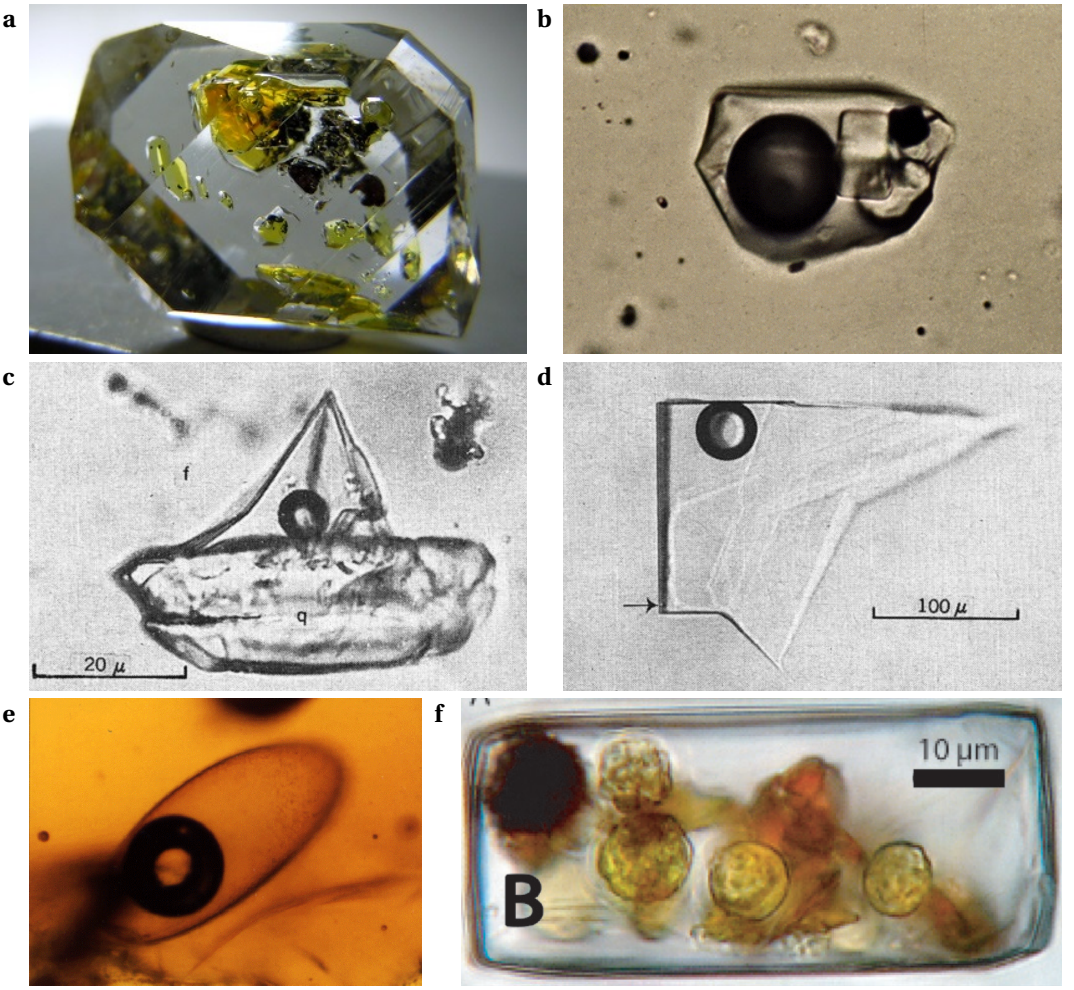

Figure 3. **a)** Petroleum inclusions (yellow) in a quartz crystal. **b)** A crowded fluid inclusion containing an aqueous solution, a gas bubble, and four minerals: halite, sylvite, gypsum, and hematite. **c)** Boat-shaped fluid inclusion left behind a quartz (q) solid inclusion formed inside fluorite (f) [18]. **d)** Bird's head-shaped fluid inclusion in fluorite [18]. **e)** Two-phase (liquid + vapor) fluid inclusion that trapped an air bubble of the 84-million-year old atmosphere. **f)** 34,000-year-old yellow algal cells in a fluid inclusion in halite from the Death Valley Core [19]. Credits: (a) Luciana Barbosa, licensed under CC By-SA 3.0; (b-e) U.S. Geological Survey; (f) Tim Lowenstein and Michael Timofeeff.

3.1. *Wonders of Nature*

Fluid inclusions are ubiquitous in minerals, being present in all kinds of rocks (sedimentary, metamorphic, and magmatic). Additionally, most ore deposits result from the precipitation of minerals from fluids in Earth's crust. Droplets of the *mother liquid* may be trapped during crystallization, forming primary inclusions. Secondary inclusions can form later, during healing of cracks in the original crystal.

Being so ubiquitous, it is not a surprise that fluid inclusions were already documented by Pliny the Elder 2000 years ago; see Refs. [15, 20, 21] for historical milestones. I will just add here

that Déodat de Dolomieu communicated in 1792 [22], 3 years before his election at the French Academy of Sciences, the observation in Florence of yellowish inclusions in quartz (similar to Figure 3 a) by his friend M. Fontana, who opened them and recognized the smell and flammability of petroleum.

Even away from the academic context, fluid inclusions have an aesthetic appeal. They may contain more than two phases (Figure 3 b), or adopt funny shapes (Figures 3 c and d). They may be very old, e.g. dating from the dinosaurs era (Figure 3 e), and even contain fossils (Figure 3 f; see also Section 3.2).

One particularly awe-striking phenomenon observable in fluid inclusions is the "perpetual" Brownian motion of some bubbles. This has been best described by the pioneer of the use of fluid inclusions in modern geology, Edwin Roedder. In his words [23]: "When the bubble is small enough to respond to statistical irregularities in the number of molecules striking it, and is free of the inclusion walls, it can be seen to wander continuously in a jerky Brownian movement. It is fascinating to watch such a bubble under the microscope and to think that it has been nervously pacing its cell for perhaps a billion years."

3.2. *Examples of use in Geosciences*

Fluid inclusions are not only fascinating natural objects. They have been used for practical purposes. By preserving information since they formed, they serve as clues for the geologist who "works like a detective in attempting to reconstruct the events of the remote past from the evidence of the present" [23]. The first among these detectives was H.C. Sorby: in his 1858 article [24], he made the connection between the homogenization temperature of the fluid inclusion (at which the bubble disappears) and the formation temperature. Even if Sorby's heritage has known ups and downs [20, 21, 25], fluid inclusions are still nowadays a major tool for geoscientists.

Any study of fluid inclusions relies on three fundamental assumptions: (i) consistency of volume ; (ii) consistency of composition ; and (iii) fluid initially trapped in a homogeneous state. Information that can be obtained from fluid inclusions falls in three broad categories. The first covers physico-chemical parameters [26]: composition (salinity, gas content), density, temperature and pressure of formation (using an equation of state and calculated isochores). The second relates to the origin of water, as deduced from the nature and concentration of the major molecules and on the isotopic composition (mainly δ^{18}O and δD). The third category encompasses the processes responsible of mineral deposition: boiling, cooling, effervescence, mixing of fluids of different origins, dilution… Fluid inclusions thus provide major input in the study of gem [27] and ore [28] formation, with obvious implications for the search of their deposits. More information about the uses of fluid inclusions can be found in specialized works [15]. For the sake of illustration, I have chosen here four examples which, albeit not among the most common studies, lead to particularly striking results.

Ice cores drilled in Antarctica [29], Greenland [30], and high mountain glaciers provide a wealth of information about past temperatures and atmospheric composition. This information is contained in the ice, through its deuterium fraction, its dust content (desert aerosols), the concentration of sodium (marine aerosol) [29, 31]. But part of it also comes from the air bubbles trapped inside ice after compaction of the initially porous top snow layer (firn) (note that, here, the trapped fluid is a gas, not a liquid). Analysis of the greenhouse gases (carbon dioxide CO_2, methane CH_4) content of the trapped air bubbles has demonstrated that "Present-day atmospheric burdens of these two important greenhouse gases seem to have been unprecedented during the past 420,000 years" [29]. Analysis of ice cores revealed rapid warming events, known as Dansgaard–Oeschger (DO) events, occuring over only a few decades [31]. The ratio of nitrogen

isotopes from the trapped air was used to reconstruct Greenland's surface temperature for the whole last glacial period, from 120 to 10 kyr ago [30], revealing temperature rises from (5 ± 3) to $16.5 \pm 3.0)$°C, which corresponds to extreme warming rates.

Past temperatures are also available from the fluid inclusions in speleothems (stalactites and stalagmites formed in caves). The ratio of hydrogen isotopes from the included water is converted into the cave air temperature. For instance, a recent study of the Milandre Cave in Switzerland [32] yields a continuous record over the past 14,000 years with a 10-20 years sample resolution. This record resembles Greenland and Mediterranean sea surface temperature trends, confirming that Europe had been cooling for the last ca. 8,000 years.

Another testimony from fluid inclusions is about seawater chemistry. Marine halites (sediments made of table salt) are deposited by seawater evaporation. Analysis of the brine trapped in halite constrains the ionic content of seawater. For instance, the Mg^{2+}/Ca^{2+} ratio has been retrieved across the whole Phanerozoic (the last 541 million years), revealing fluctuations "in phase with oscillations in seafloor spreading rates, volcanism, global sea level, and the primary mineralogies of marine limestones and evaporites" [33]. A threefold increase in Ca^{2+} concentration has been observed during the Early Cambrian (ca. 515 million years ago) [34], which may have been the cause of the sudden onset of biomineralization, and played a role in the major evolutionary change known as the "Cambrian explosion", when the major *phyla* of today's pluricellular organisms emerged.

Fluid inclusions do not only preserve physical information, but also organic compounds, microorganisms, and even life. Indeed, microorganisms can be seen inside fluid inclusions in rock salt (see for instance Fig. 3 f), some as old as 830-million-year [35]. Bacteria could be recovered from fluid inclusions, and their DNA sequenced: e.g. ribosomal DNA of a 250-million-year-old specimen [36], or complete genome for a 123-million-year-old one [37]; the cells could even be cultured and multiplied. Such discoveries are not without controversy, about possible contamination and the surprising preservation of DNA for such long period of times [19]. Still, suitable sterilization protocols have been demonstrated [38], and half-a-million-year-old bacteria from the permafrost show evidence for active DNA repair [39]. This gives confidence in results obtained from fluid inclusions following the best practices. Extending the time travel to as far as 3.5-billion-year in the past, the primary ingredients for life (small molecules such as hydrogen sulfide, carbonyl sulfide, methane, acetic acid…) have been detected in fluid inclusions in Australian rocks [40]. Based on the successful achievements on Earth, it is now envisioned to search for past life on Mars by examining fluid inclusions in its sediments [41].

4. Fluid inclusions: a tool for studying stretched water

Extensively used by geoscientists, inclusions are also intimately linked to the study of water. Ice exists among various possible crystalline phases: 19 ice polymorphs are known to date [42]). Two of them, ice VI and VII, stable at high pressure, exist in the deep Earth. They have also been found at the surface, preserved as solid inclusions in diamond [43, 44]. In this section, we focus on fluid inclusions, which have become a device to bring water to negative pressure, and study its properties. We first explain the principle of the Berthelot tube, which allows stretching water (Section 4.1), and we present the first uses of fluid inclusions as microscopic Berthelot tubes (Section 4.2). Then we describe recent achievements in the statistics of nucleation (Section 4.3) and the equation of state of stretched water (Section 4.4).

4.1. *The Berthelot tube method*

In 1850, Berthelot discovered a way to stretch a liquid by nearly-isochoric cooling, which was presented at the French Academy of Sciences, in the session held on June 24, 1850 [45]; the full

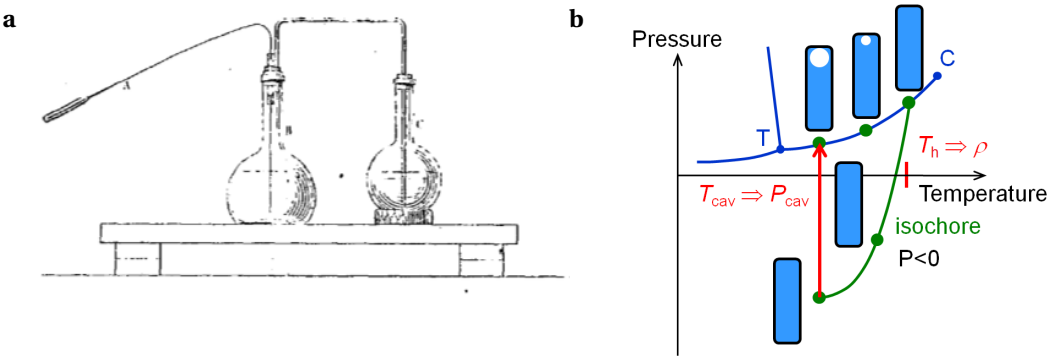

Figure 4. a) Original tube (A) used by Marcellin Berthelot [45]. **b)** Principle of the Berthelot tube method.

memoir was published in October 1850. Figure 4 a shows a sketch of Berthelot's setup to fill a thick-walled tube with a liquid under its vapor pressure, before sealing it with a flame. Figure 4 b explains the method. Initially, the liquid is in equilibrium with a small vapor bubble in a closed container. Warming along the liquid-vapor equilibrium (blue curve joining the triple point T to the critical point C), the bubble shrinks until it disappears at temperature T_h, from which the density ρ of the liquid filling the container is determined. Then, upon cooling, the bubble does not reappear immediately, so that the liquid now occupies a larger volume than when the bubble was present: the liquid is stretched, and may reach negative pressure. For a perfectly rigid vessel, the liquid would follow an isochore (green curve); thermal expansion and elastic deformation may cause the exact path to deviate from a strict isochore. If the tension becomes large enough, a vapor bubble nucleates at T_{cav} and the system goes back to liquid-vapor equilibrium. Berthelot estimated $P_{cav} = -5$ MPa at 18°C. We will not review all subsequent attempts (see Ref. [5]), but jump to the noteworthy work by Henderson and Speedy, who provided a direct determination of the line of density maximum of water at negative pressure [46]. They improved a setup first used by Meyer [47], in which the container is given the shape of an helix, becoming a Bourdon gauge: the degree of winding or unwinding of the helix gives (after calibration) the pressure in the liquid. The maximum tension is reached when the thermodynamic path crosses the line of density maximum of water, which is at 4°C at ambient pressure. With the Berthelot–Bourdon method, the density maximum was found to occur at 8.3°C at −20.3 MPa. Unfortunately, all attempts with these still relatively large Berthelot tubes reached less negative values than (or at best similar to) acoustic methods, thus falling short of the large negative P_{cav} theoretically predicted (Figure 1 b).

4.2. *Fluid inclusions as microscopic Berthelot tubes*

Roedder noticed the large degree of supercooling that could be reached in fluid inclusions [48]. Based on a first observation by John P. Creel of ice crystals above 0°C, Roedder also followed ice-liquid equilibrium at negative pressure. He observed ice at 6.5°C, at which he estimated the negative pressure to exceed –90 MPa [49]. The record was only recently beaten by Qiu et al. who observed ice melting at 6.8°C [50].

Thus, water in fluid inclusions seems to be the sample of choice for approaching the theoretical limit for cavitation (Section 2.3). This was conjectured by Angell et al., who indeed observed extreme tensions first in salty solutions [51] and then in pure water [4]. The pressure, estimated from the density obtained from the homogenization temperature and from the cavitation temperature, are shown in Figure 1 b. For the best samples, the results do indeed follow the theoretical

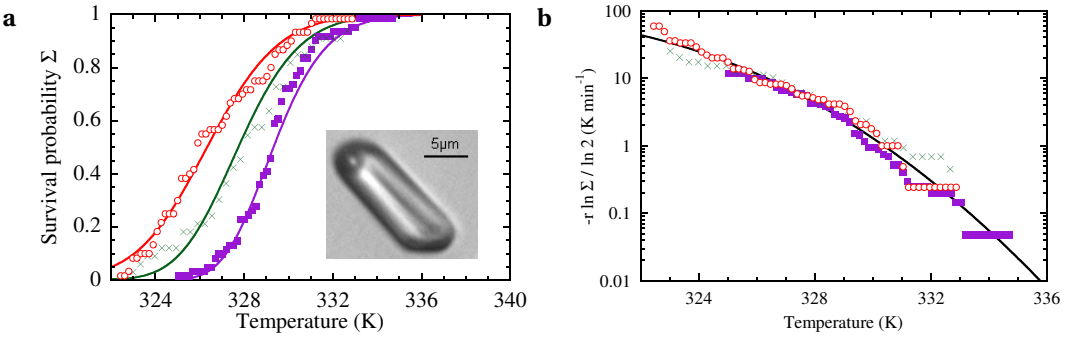

Figure 5. a) Survival probability Σ of the metastable liquid in the fluid inclusion (inset) when cooling at three different rates (r = 2, 5, and 10 K min^{-1} shown with purple squares, green crosses, and red circles, respectively). **b)** When plotting $-r \ln\Sigma / \ln 2$, the three sets of data collapse, as expected from nucleation theory [53].

prediction, and pressures beyond −120 MPa are within reach. The technique has been extended to solutions by preparing synthetic inclusions containing various salts, in which large tensions are also obtained [52].

4.3. *Statistics of bubble nucleation*

Angell et al. [4] measured the cavitation temperature T_{cav} in many inclusions. The various liquid density used yielded a large range of T_{cav} values. Even in a given sample containing several inclusions with the same liquid density, various values of T_{cav} were observed, with only some close to the predicted nucleation limit.

We decided to use a complementary approach. Instead of measuring many inclusions once, we selected one good fluid inclusion (reaching an extreme cavitation pressure), and measured its T_{cav} 166 times [53]. As cavitation is a stochastic phenomenon, the distribution of T_{cav} shows a finite width, even for the same inclusion (see Figure 5 a). The average T_{cav} also shows a dependence on the cooling rate. We found that the detailed T_{cav} distribution showed a shape and a cooling rate dependence following expectations from nucleation theory (Figure 5 b). This allowed us to provide a new piece of information about cavitation in water. The nucleation rate derived from the measured distribution was analyzed thanks to the nucleation theorem [54] to obtain the size of the critical bubble involved in nucleation. Our estimate is around 5 nm^3. This nanoscopic size is in line with theoretical predictions. It is remarkable that measurements based on observations made with an optical microscope and a standard camera are able to give information about a nanoscopic event occurring in less than a nanosecond.

4.4. *The equation of state at negative pressure*

After learning about the limit at which liquid water breaks, we started to measure its properties before it breaks. While the confined nature of a fluid inclusion does not allow to easily insert a sensor, it provides the only method able to approach the homogeneous cavitation limit (see Section 2.3). We had therefore to resort to a non-intrusive technique. Quartz being transparent, an optical technique was in order. High pressure scientists meet the same constraints when they want to determine properties of substances brought at extreme pressures in the diamond anvil cell. They often resort to Brillouin spectroscopy to locate phase transitions or obtain equations of

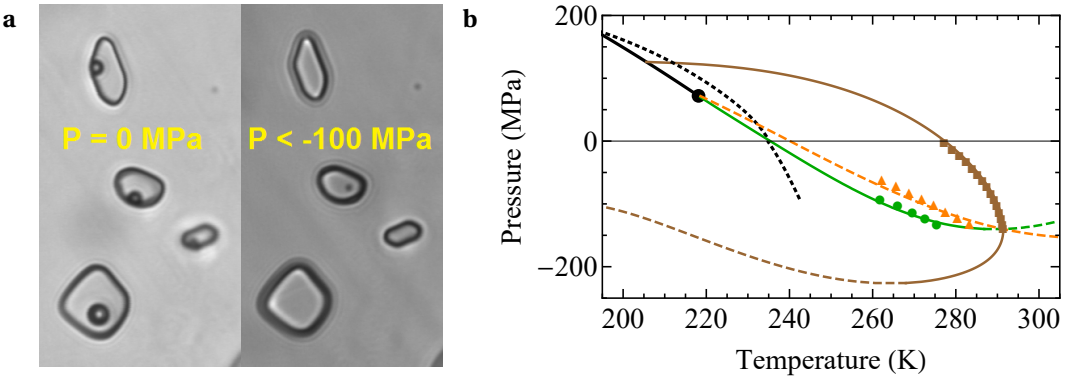

Figure 6. a) Fluid inclusions for the equation of state of water at liquid-vapor equilibrium (bubble present, left) and at negative pressure (homogeneous liquid, right) [57]. **b)** Remarkable lines in the phase diagram of water, from a two-state model [58]. The black line shows the putative liquid-liquid transition, terminating at a liquid-liquid critical point (black disc). The short-dashed black curve shows the line of homogeneous ice nucleation [50,59–61]. The lines of maxima and minima for the model are shown with solid and dashed curves, respectively, for density (brown), isothermal compressibility (green), and sound velocity (orange) extrema along isobars. The symbols show the corresponding experimental extrema reported by Holten *et al.* [57] for density (brown squares), isothermal compressibility (green discs), and sound velocity (orange triangles).

state; see e.g. Refs. [55] and [56], respectively, for examples with water. Brillouin light scattering is the inelastic interaction between light and matter. A laser passing through the liquid can absorb or generate density waves; the photons thus gain or lose energy, respectively, which reflects in a shift in the light frequency, proportional to the sound velocity in the liquid. The shift is tiny, typically a few parts per million, but can be accurately measured with a Fabry–Pérot interferometer. Using systematic measurements at various pressures and temperatures, thermodynamic integration allows the calculation of the density, thus yielding a non intrusive way to measure an equation of state. This approach has been used for instance on aqueous NaCl solutions to 1073K and 4.5 GPa [56].

Alvarenga et al. [62] made an early attempt to apply the Brillouin technique to water inclusions in quartz. While their study confirmed the order of magnitude of the pressure obtained by Angell based on an extrapolated equation of state, they did not try to derive an experimental one. We decided to build a Brillouin micro-spectrometer to tackle this question. In a series of works [57, 63, 64], we obtained the sound velocity in metastable fluid inclusions (some of them are shown in Figure 6 a). Our study revealed new anomalies of the sound velocity in cold stretched water. The sound velocity departs significantly from the extrapolation of the equation of state based on positive pressure data [65]. We were able to follow the line of density maximum: the temperature at which the maximum density is reached monotonically increases from 4 to 18°C when the pressure decreases from ambient to −137 MPa [57].

We also discovered a new anomaly at low temperature and large negative pressure: the existence of isothermal compressibility maxima along isobars. This is of utmost importance in the debate about the origin of water's anomalies. First based on molecular dynamics simulations [66], it has been proposed that supercooled water could exist as two distinct liquid phases. This surprising phenomenon is known as liquid polyamorphism. The two putative liquids would coexist along a first-order transition line, terminating at a liquid-liquid critical point. This second critical

point (in addition to the usual one terminating the liquid-vapor transition) would be the common origin for the anomalies of water (see Ref. [67] for a review of this and other scenarios). Observation of the two liquids for a short duration has been recently reported [68]. The existence of isothermal compressibility maxima along isobars is a necessary but not sufficient condition for the liquid-liquid critical point to exist. Our results at negative pressure are thus consistent with such a critical point, although they do not definitely prove its existence.

We have combined our data at negative pressure with literature values at positive pressure in a comprehensive fit of thermodynamic data for water [58]. We adopted a two-state description of water, as a non-ideal mixture of two interconverting species (see Refs. [69, 70] for reviews). Depending on the degree of non-ideality, such a model may predict that water separates in two distinct liquid phases at low temperatures. Our fit with the two state model [58] places the critical coordinates at 218 K and 72 MPa. Figure 6b displays the observed lines of anomalies in water, their extrapolation, and the predicted liquid-liquid transition.

We recently started to apply the Brillouin method to salt solutions [71], in order to measure the effect of solutes on water's anomalies.

5. Back to Earth: palaeotemperature

The day I started writing this article, Thomas Pesquet came back to Earth after 199 days in the International Space Station[1]. It's now time for me to explain how, more modestly, after 10 years spent in the depths of the properties of water at negative pressure, I tried to emerge back to more earthly matters.

5.1. *The problem with evaporites*

An evaporite is a sedimentary rock that originates from evaporation of a saline water reservoir in a closed basin. They are ubiquitous on Earth, being found over a broad range of latitudes and altitudes [16]. Evaporites deposited throughout Earth history, from at least 1 billion year ago [72] until today (e.g. in the Dead Sea). The evaporitic crystals often contain fluid inclusions. If primary and intact, reading the entrapment temperature from the fluid properties would offer an invaluable testimony about past temperatures. Attempts in that direction have been made, based on the homogenization temperature T_h (Section 4.1): if the fluid was trapped near ambient pressure, when the crystal closed around a cavity filled with liquid, the vapor bubble in the fluid inclusion should disappear at the entrapment temperature. One common issue is the absence of bubble in the fluid inclusion in low temperature geological environment (e.g. ambient conditions). The liquid may have cooled since entrapment, reaching a metastable state, but only a mild one, so that bubble nucleation is unlikely to occur, even over geological times. This renders microthermometry useless, as determining T_h requires a bubble. Researchers noticed that cooling the sample to low enough temperatures, e.g. in a freezer, made the bubble appear in some inclusions, thus giving a new hope to get results from microthermometry [73]. Unfortunately, in a detailed study of synthetic and natural NaCl crystals grown at a known temperature, Lowenstein et al. [74] have shown that T_h obtained after cold treatment have erratic values, biased towards low temperatures. This is likely due to irreversible deformation of the fluid inclusion during the temperature cycle [75]. Lowenstein et al. suggested to use the maximum observed T_h as a proxy for the actual entrapment temperature. But the result may change if more inclusions are measured, and the number of possible measurements is itself limited by the fact that only a fraction of the inclusions show a bubble after cooling. Since then, fluid inclusions

[1] https://www.nytimes.com/2021/11/09/science/spacex-nasa-water-landing.html

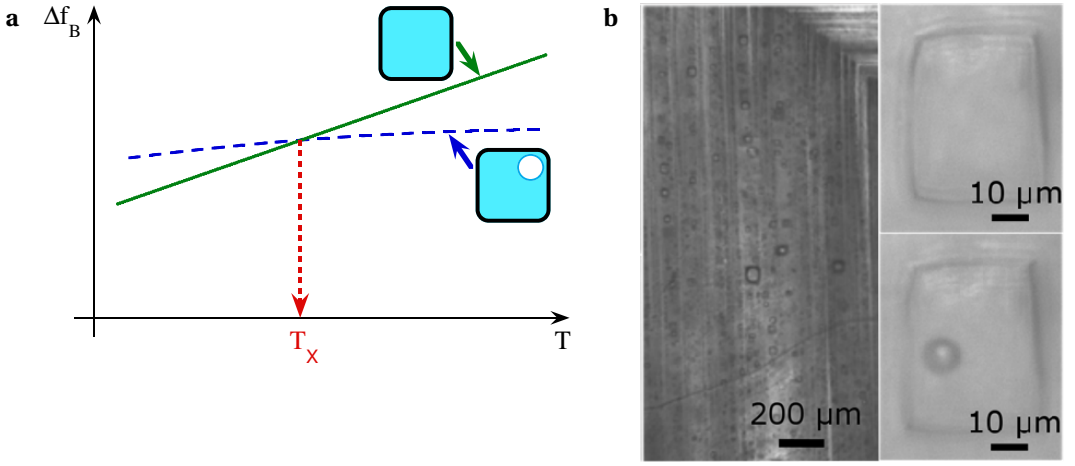

Figure 7. a) Principle of the reconstruction of entrapment temperature from Brillouin spectroscopy. The Brillouin frequency shift Δf_B is measured as a function of temperature T in the monophasic inclusion (green solid curve) and, after nucleating a bubble using a large thermal excursion, along liquid-vapor equilibrium (blue dashed curve); the two curves cross at T_x, which corresponds to the entrapment temperature for samples grown at pressures near ambient. **b)** Examples of fluid inclusions in halite from the Dead Sea.

have been used in palaeotemperature studies, but without a clear consensus about the best data analysis (see Ref. [75] and references therein).

An additional complication has been pointed out [76–79]. The bubble surface being curved, the pressure in the vapor is higher than in the liquid, because of the Laplace pressure jump ΔP due to surface tension σ: $\Delta P = 2\sigma/R$ for a spherical bubble with radius R. The smaller the bubble, the larger ΔP, so that the observed T_h is lower than if surface tension could be neglected. Moreover, the energy cost associated with the liquid-vapor interface ($4\pi R^2\sigma$) is sometimes larger in absolute value than the gain in energy associated with releasing the tension in the liquid. In that paradoxical case, even if a bubble appears, it will immediately disappear and the fluid inclusion will remain permanently filled with liquid. This precludes any measurement of T_h.

5.2. *The Brillouin palaeothermometer*

How can we overcome the limitations listed in the previous section? To nucleate a vapor bubble without the need for a freezer, Krüger et al. have used focused femtosecond laser pulses [80]. They applied this technique to perform microthermometry on inclusions in stalagmites [78] and gypsum [81]. After correction of the Laplace pressure effect, the T_h for inclusions in stalagmites was found to agree with the monitored cave temperature in which they grew. However, the Laplace correction requires an accurate measurement of the bubble volume and theoretical modeling; it also assumes the surface tension of pure water and neglects thermal fluctuations that can make the bubble disappear at even lower temperature. In cases where the bubble is always unstable (see Section 5.1), the technique simply does not work.

We have proposed another method based on Brillouin spectroscopy (see Section 4.4), whose principle is illustrated in Figure 7 a. The Brillouin frequency shift Δf_B is proportional to the sound velocity in the liquid, which depends on its composition, and also on the temperature T and pressure path followed by the fluid. When the fluid inclusion is monophasic (filled with liquid), the

liquids follows a quasi-isochore (nearly constant volume). When a bubble is present (biphasic inclusion after cavitation), the system is at liquid-vapor equilibrium. The two corresponding curves for $\Delta f_B(T)$ cross when the monophasic fluid inclusion reaches the temperature at which it would be in equilibrium with vapor. We thus identify the intersection of the two $\Delta f_B(T)$ curves as T_h. For fluid inclusions in quartz, bubble nucleation occurs systematically at low enough fluid density, and yields reproducible T_h values with microthermometry. We thus first tested the Brillouin method on quartz samples, and found an excellent agreement with microthermometry [82].

For halite, as explained in Section 5.1, bubbles are more difficult to obtain. We implement the method as follows. We first measure $\Delta f_B(T)$ in the monophasic inclusion, in a small temperature range around the expected entrapment temperature, thus avoiding any plastic deformation. Then, we trigger bubble nucleation. We found for halite a way to systematically obtain a bubble, by warming the sample up to 130°C. The large pressure increase in the inclusion induces its irreversible expansion, so that the mechanical tension that builds up when cooling the liquid to room temperature is now large enough to trigger bubble nucleation. The sample is obviously damaged, but this is not an issue, as the measured $\Delta f_B(T)$ still follows the same liquid-vapor equilibrium curve, even if the total inclusion volume is larger.

We tested the method on lab-grown samples, made by evaporation of solutions of NaCl in ultrapure water under controlled temperature. The Brillouin technique recovered the growth temperature within better than 1°C, provided that small and isolated inclusions were selected [75]. Indeed, the elastic limit of the salt crystal is much less than for quartz, and large inclusions or inclusions close to others or to the crystal surface easily deform, even in the first measurement step involving only moderate departure from the growth temperature. The Brillouin method also presents a significant advantage over microthermometry: as the bubble appearance occurs systematically, good statistics can be obtained, and the average of measurements used, instead of the maximum value of a small set of microthermometry data.

We are now using the Brillouin palaeothermometer on an evaporitic sequence of a sedimentary core retrieved in the modern Dead Sea Basin (Figure 7b), that encloses a succession of glacial-interglacial cycles covering the last 200,000 years. We believe our data will provide new insight on the climate during the last Interglacial [75, 83]. Halite layers in the sedimentary core exhibit a fine structure with an alternation of coarse and fine crystals layers. By analogy with the modern halite precipitation mechanism [84], coarse layers correspond to crystals growing at the lake bottom during spring to late summer, and fine layers to cumulate halite precipitating in the whole water column mainly during winter, and to a minor extent during summer. By sampling crystals at different heights in a given coarse layer, we resolve temperature changes during the layer growth. We have thus revealed a recurring increase of entrapment temperatures for three consecutive years (*ca.* 130 kyr ago) by 3.0, 4.6, and 1.5°C, respectively [85]. This is between 1 to 3 times the measured modern temperature change of the lake bottom, 1.5°C for the 1996-2010 period.

6. Conclusion

Stretched water, known to Huygens and studied by Berthelot, can still bring about new discoveries. Thanks in particular to Austen Angell, fluid inclusions, which are tools familiar to geoscientists, have been turned into the only tractable method to bring water close to its homogeneous cavitation limit. We have heavily relied on it to study the anomalies of water. We thus determined the line of density maxima down to −137 MPa, and provided the first evidence for a maximum of isothermal compressibility along isobars.

After borrowing their tool, it was natural to give it back to geoscientists, with a thank-you bonus. This lead us to develop a new method for palaeotemperature reconstruction from fluid

inclusions. We hope we have brought again into light these silent witnesses of the past climate, and found a way to make them tell their story.

Conflicts of interest

The author has no conflict of interest to declare.

Acknowledgments

I wish to thank all my co-authors for their contributions troughout the years. I thank in particular: Véronique Gardien for opening me the gates of geosciences; Mouna El Mekki-Azouzi, Chandra Shekhar Pati Tripathi, and Gaël Pallares for giving a proof-of-principle of Brillouin thermometry using inclusions in quartz; Emmanuel Guillerm for making the Brillouin palaeothermometer a reality; and Niels Brall for adding the seasonal dimension. I acknowledge helpful input from Thomas Loerting and Emmanuel Guillerm when preparing this manuscript. I thank the Ecole de Physique des Houches for giving me the opportunity to co-organize with Abraham Stroock the workshop *Metastability and nucleation in water: theory, experiments, and applications*, 1-6 June 2014, which gathered 64 scientists coming from physics, chemistry, engineering, earth science, and biology[2]. I am indebted to Pablo G. Debenedetti, Mikhail A. Anisimov, and to late C. Austen Angell for their continuous encouragements.

References

[1] M. T. Tyree, M. H. Zimmermann, *Xylem Structure and the Ascent of Sap*, 2nd ed., Springer Series in Wood Science, Springer, 2002.
[2] H. Cochard, "Cavitation in Trees", *Comptes Rendus Phys.* **7** (2006), no. 9-10, p. 1018-1026.
[3] E. Herbert, S. Balibar, F. Caupin, "Cavitation Pressure in Water", *Phys. Rev. E* **74** (2006), no. 4, article no. 041603.
[4] Q. Zheng, D. J. Durben, G. H. Wolf, C. A. Angell, "Liquids at Large Negative Pressures: Water at the Homogeneous Nucleation Limit", *Science* **254** (1991), no. 5033, p. 829-832.
[5] F. Caupin, E. Herbert, "Cavitation in Water: A Review", *Comptes Rendus Physique* **7** (2006), no. 9-10, p. 1000-1017.
[6] J. C. Fisher, "The Fracture of Liquids", *J. Appl. Phys.* **19** (1948), no. 11, p. 1062-1067.
[7] P. G. Debenedetti, *Metastable Liquids: Concepts and Principles*, Princeton University Press, 1996.
[8] D. W. Oxtoby, "Nucleation of First-Order Phase Transitions", *Acc. Chem. Res.* **31** (1998), no. 2, p. 91-97.
[9] C. Huygens, "Extrait d'une Lettre de M. Hugens de l'Académie Royale Des Sciences à l'auteur de Ce Journal, Touchant Les Phénomènes de l'eau Purgée d'air", *J. Sçavans* (1672).
[10] C. Huygens, "An Extract of a Letter of M. Hugens to the Author of the Journal Des Scavans of July 25. 1672. Attempting to Render the Cause of That Odd Phaenomenon of the QuickSilvers Remaining Suspended Far above the Usual Height in the Torricellian Experiments", *Philos. Trans. 1665-1678* **7** (1672), p. 5027-5030.
[11] G. S. Kell, "Early Observations of Negative Pressures in Liquids", *Am. J. Phys.* **51** (1983), no. 11, p. 1038-1041.
[12] F. Caupin, A. D. Stroock, "The Stability Limit and Other Open Questions on Water at Negative Pressure", in *Liquid Polymorphism: Advances in Chemical Physics* (H. E. Stanley, S. Rice, eds.), no. 152, John Wiley & Sons, 2013, p. 51-80.
[13] K. Davitt, A. Arvengas, F. Caupin, "Water at the Cavitation Limit: Density of the Metastable Liquid and Size of the Critical Bubble", *Eur. Phys. Lett.* **90** (2010), no. 1, article no. 16002.
[14] A. Arvengas, K. Davitt, F. Caupin, "Fiber Optic Probe Hydrophone for the Study of Acoustic Cavitation in Water", *Rev. Sci. Instrum.* **82** (2011), no. 3, article no. 034904.
[15] V. Hurai, M. Huraiová, M. Slobodník, R. Thomas, *Geofluids: Developments in Microthermometry, Spectroscopy, Thermodynamics, and Stable Isotopes*, Elsevier, 2015.
[16] J. K. Warren, *Evaporites – a Geological Compendium*, Springer, 2016.
[17] E. Roedder, *Fluid Inclusions*, Reviews in Mineralogy & Geochemistry, vol. 12, Walter de Gruyter, 2018, Ebook version of the 1984 edition.
[18] E. Roedder, A. V. Heyl, J. P. Creel, "Environment of Ore Deposition at the Mex-Tex Deposits, Hansonburg District, New Mexico, from Studies of Fluid Inclusions", *Econ. Geol.* **63** (1968), no. 4, p. 336-348.

[2] https://water2014.sciencesconf.org/

[19] T. K. Lowenstein, B. A. Schubert, M. N. Timofeeff, "Microbial Communities in Fluid Inclusions and Long-Term Survival in Halite", *GSA Today* **21** (2011), no. 1, p. 4-9.
[20] M. Dubois, "Les Grandes Étapes Du Développement de l'étude Des Inclusions Fluides", *Trav. Com. Fr. Hist. Geol.* **17** (2003), p. 1-22.
[21] S. E. Kesler, R. J. Bodnar, T. P. Mernagh, "Role of Fluid and Melt Inclusion Studies in Geologic Research", *Geofluids* **13** (2013), no. 4, p. 398-404.
[22] D. de Dolomieu, "Sur de l'huile de Pétrole Dans Le Cristal de Roche et Les Fluides Élastiques Tirés Du Quartz", *J. Phys. Chim. Hist. Nat. Arts* **40** (1792).
[23] E. Roedder, "Ancient Fluids in Crystals", *Sci. Am.* **207** (1962), no. 4, p. 38-47.
[24] H. C. Sorby, "On the Microscopical, Structure of Crystals, Indicating the Origin of Minerals and Rocks", *Q. J. Geol. Soc.* **14** (1858), no. 1-2, p. 453-500.
[25] J. L. R. Touret, "Les inclusions fluides : histoire d'un paradoxe", *Bull. Minéralogie* **107** (1984), no. 2, p. 125-137.
[26] J. L. R. Touret, "Fluids in Metamorphic Rocks", *Lithos* **55** (2001), no. 1-4, p. 1-25.
[27] G. Giuliani, J. Dubessy, D. Ohnenstetter, D. Banks, Y. Branquet, J. Feneyrol, A. E. Fallick, J.-E. Martelat, "The Role of Evaporites in the Formation of Gems during Metamorphism of Carbonate Platforms: A Review", *Miner. Depos.* **53** (2018), no. 1, p. 1-20.
[28] P. Voudouris, C. Mavrogonatos, P. G. Spry, T. Baker, V. Melfos, R. Klemd, K. Haase, A. Repstock, A. Djiba, U. Bismayer, A. Tarantola, C. Scheffer, R. Moritz, K. Kouzmanov, D. Alfieris, K. Papavassiliou, A. Schaarschmidt, E. Galanopoulos, E. Galanos, J. Kołodziejczyk, C. Stergiou, M. Melfou, "Porphyry and Epithermal Deposits in Greece: An Overview, New Discoveries, and Mineralogical Constraints on Their Genesis", *Ore Geology Reviews* **107** (2019), p. 654-691.
[29] J. R. Petit, J. Jouzel, D. Raynaud, N. I. Barkov, J.-M. Barnola, I. Basile, M. Bender, J. Chappellaz, M. Davis, G. Delaygue, M. Delmotte, V. M. Kotlyakov, M. Legrand, V. Y. Lipenkov, C. Lorius, L. Pépin, C. Ritz, E. Saltzman, M. Stievenard, "Climate and Atmospheric History of the Past 420,000 Years from the Vostok Ice Core, Antarctica", *Nature* **399** (1999), no. 6735, p. 429-436.
[30] P. Kindler, M. Guillevic, M. Baumgartner, J. Schwander, A. Landais, M. Leuenberger, "Temperature Reconstruction from 10 to 120 kyr b2k from the NGRIP Ice Core", *Clim. Past* **10** (2014), no. 2, p. 887-902.
[31] R. B. Alley, "Ice-Core Evidence of Abrupt Climate Changes", *Proc. Natl. Acad. Sci. USA* **97** (2000), no. 4, p. 1331-1334.
[32] S. Affolter, A. Häuselmann, D. Fleitmann, R. L. Edwards, H. Cheng, M. Leuenberger, "Central Europe Temperature Constrained by Speleothem Fluid Inclusion Water Isotopes over the Past 14,000 Years", *Sci. adv.* **5** (2019), no. 6, article no. eaav3809.
[33] T. K. Lowenstein, M. N. Timofeeff, S. T. Brennan, L. A. Hardie, R. V. Demicco, "Oscillations in Phanerozoic seawater chemistry: evidence from fluid inclusions", *Science* **294** (2001), no. 5544, p. 1086-1088.
[34] S. T. Brennan, T. K. Lowenstein, J. Horita, "Seawater Chemistry and the Advent of Biocalcification", *Geology* **32** (2004), no. 6, p. 473-476.
[35] S. I. Schreder-Gomes, K. C. Benison, J. A. Bernau, "830-Million-Year-Old Microorganisms in Primary Fluid Inclusions in Halite", *Geology* **50** (2022), no. 8, p. 918-922.
[36] R. H. Vreeland, W. D. Rosenzweig, D. W. Powers, "Isolation of a 250 Million-Year-Old Halotolerant Bacterium from a Primary Salt Crystal", *Nature* **407** (2000), no. 6806, p. 897-900.
[37] S. T. Jaakkola, F. Pfeiffer, J. J. Ravantti, Q. Guo, Y. Liu, X. Chen, H. Ma, C. Yang, H. M. Oksanen, D. H. Bamford, "The Complete Genome of a Viable Archaeum Isolated from 123-Million-Year-Old Rock Salt", *Environ. Microbiol.* **18** (2016), no. 2, p. 565-579.
[38] K. Sankaranarayanan, M. N. Timofeeff, R. Spathis, T. K. Lowenstein, J. K. Lum, "Ancient Microbes from Halite Fluid Inclusions: Optimized Surface Sterilization and DNA Extraction", *PLOS ONE* **6** (2011), no. 6, article no. e20683.
[39] S. S. Johnson, M. B. Hebsgaard, T. R. Christensen, M. Mastepanov, R. Nielsen, K. Munch, T. Brand, M. T. P. Gilbert, M. T. Zuber, M. Bunce, R. Rønn, D. Gilichinsky, D. Froese, E. Willerslev, "Ancient Bacteria Show Evidence of DNA Repair", *Proc. Natl. Acad. Sci.* **104** (2007), no. 36, p. 14401-14405.
[40] H. Mißbach, J.-P. Duda, A. M. van den Kerkhof, V. Lüders, A. Pack, J. Reitner, V. Thiel, "Ingredients for Microbial Life Preserved in 3.5 Billion-Year-Old Fluid Inclusions", *Nat. Commun.* **12** (2021), no. 1, p. 1101.
[41] K. C. Benison, "How to Search for Life in Martian Chemical Sediments and Their Fluid and Solid Inclusions Using Petrographic and Spectroscopic Methods", *Front. Environ. Sci.* **7** (2019), article no. 108.
[42] T. Loerting, V. Fuentes-Landete, C. M. Tonauer, T. M. Gasser, "Open Questions on the Structures of Crystalline Water Ices", *Commun. Chem.* **3** (2020), no. 1, p. 109.
[43] H. Kagi, R. Lu, P. Davidson, A. F. Goncharov, H. K. Mao, R. J. Hemley, "Evidence for Ice VI as an Inclusion in Cuboid Diamonds from High P-T near Infrared Spectroscopy", *Mineral. Mag.* **64** (2000), no. 6, p. 1089-1097.
[44] O. Tschauner, S. Huang, E. Greenberg, V. B. Prakapenka, C. Ma, G. R. Rossman, A. H. Shen, D. Zhang, M. Newville, A. Lanzirotti, K. Tait, "Ice-VII Inclusions in Diamonds: Evidence for Aqueous Fluid in Earth's Deep Mantle", *Science* **359** (2018), no. 6380, p. 1136-1139.
[45] M. Berthelot, "Sur Quelques Phénomènes de Dilatation Forcée Des Liquides", *Ann. Chim. Phys.* **30** (1850), p. 232-237.

[46] S. J. Henderson, R. J. Speedy, "Temperature of Maximum Density in Water at Negative Pressure", *J. Phys. Chem.* **91** (1987), no. 11, p. 3062-3068.
[47] J. Meyer, "Zur Kenntnis Des Negativen Druckes in Flüssigkeiten", *Abh. Dtsch. Bunsen–Gessellschaft* **6** (1911), p. 1-53.
[48] E. Roedder, "Studies of Fluid Inclusions; Part 1, Low Temperature Application of a Dual-Purpose Freezing and Heating Stage", *Econ. Geol.* **57** (1962), no. 7, p. 1045-1061.
[49] E. Roedder, "Metastable Superheated Ice in Liquid-Water Inclusions under High Negative Pressure", *Science* **155** (1967), no. 3768, p. 1413-1417.
[50] C. Qiu, Y. Krüger, M. Wilke, D. Marti, J. Rička, M. Frenz, "Exploration of the Phase Diagram of Liquid Water in the Low-Temperature Metastable Region Using Synthetic Fluid Inclusions", *Phys. Chem. Chem. Phys.* **18** (2016), no. 40, p. 28227-28241.
[51] J. L. Green, D. J. Durben, G. H. Wolf, C. A. Angell, "Water and Solutions at Negative Pressure: Raman Spectroscopic Study to -80 Megapascals", *Science* **249** (1990), no. 4969, p. 649-652.
[52] K. I. Shmulovich, L. Mercury, R. Thiéry, C. Ramboz, M. El Mekki, "Experimental Superheating of Water and Aqueous Solutions", *Geochim. Cosmochim. Acta* **73** (2009), no. 9, p. 2457-2470.
[53] M. E. M. Azouzi, C. Ramboz, J.-F. Lenain, F. Caupin, "A Coherent Picture of Water at Extreme Negative Pressure", *Nat. Phys.* **9** (2012), no. 1, p. 38-41.
[54] D. W. Oxtoby, D. Kashchiev, "A General Relation between the Nucleation Work and the Size of the Nucleus in Multicomponent Nucleation", *J. Chem. Phys.* **100** (1994), no. 10, p. 7665-7671.
[55] A. Polian, M. Grimsditch, "Brillouin Scattering from H_2O: Liquid, Ice VI, and Ice VII", *Phys. Rev. B* **27** (1983), no. 10, p. 6409-6412.
[56] D. Mantegazzi, C. Sanchez-Valle, T. Driesner, "Thermodynamic Properties of Aqueous NaCl Solutions to 1073 K and 4.5 GPa, and Implications for Dehydration Reactions in Subducting Slabs", *Geochim. Cosmochim. Acta* **121** (2013), p. 263-290.
[57] V. Holten, C. Qiu, E. Guillerm, M. Wilke, J. Rička, M. Frenz, F. Caupin, "Compressibility Anomalies in Stretched Water and Their Interplay with Density Anomalies", *J. Phys. Chem. Lett.* **8** (2017), no. 22, p. 5519-5522.
[58] F. Caupin, M. A. Anisimov, "Thermodynamics of Supercooled and Stretched Water: Unifying Two-Structure Description and Liquid-Vapor Spinodal", *J. Chem. Phys.* **151** (2019), no. 3, article no. 034503.
[59] H. Kanno, R. J. Speedy, C. A. Angell, "Supercooling of Water to −92 °C under Pressure", *Science* **189** (1975), no. 4206, p. 880-881.
[60] H. Kanno, K. Miyata, "The Location of the Second Critical Point of Water", *Chem. Phys. Lett.* **422** (2006), no. 4-6, p. 507-512.
[61] V. Holten, J. V. Sengers, M. A. Anisimov, "Equation of State for Supercooled Water at Pressures up to 400 MPa", *J. Phys. Chem. Ref. Data* **43** (2014), no. 4, article no. 043101.
[62] A. D. Alvarenga, M. Grimsditch, R. J. Bodnar, "Elastic Properties of Water under Negative Pressures", *J. Chem. Phys.* **98** (1993), no. 11, p. 8392-8396.
[63] G. Pallares, M. E. M. Azouzi, M. A. González, J. L. Aragones, J. L. F. Abascal, C. Valeriani, F. Caupin, "Anomalies in Bulk Supercooled Water at Negative Pressure", *Proc. Natl. Acad. Sci. USA* **111** (2014), no. 22, p. 7936-7941.
[64] G. Pallares, M. A. Gonzalez, J. L. F. Abascal, C. Valeriani, F. Caupin, "Equation of State for Water and Its Line of Density Maxima down to -120 MPa", *Phys. Chem. Chem. Phys.* **18** (2016), no. 8, p. 5896-5900.
[65] The International Association for the Properties of Water and Steam, "Revised release on the IAPWS formulation 1995 for the thermodynamic properties of ordinary water substance for general and scientific use", Tech. Report IAPWS R6-95(2018), The International Association for the Properties of Water and Steam, 2018, http://www.iapws.org/relguide/IAPWS95-2018.pdf.
[66] P. H. Poole, F. Sciortino, U. Essmann, H. E. Stanley, "Phase Behaviour of Metastable Water", *Nature* **360** (1992), no. 6402, p. 324-328.
[67] P. Gallo, K. Amann-Winkel, C. A. Angell, M. A. Anisimov, F. Caupin, C. Chakravarty, E. Lascaris, T. Loerting, A. Z. Panagiotopoulos, J. Russo, J. A. Sellberg, H. E. Stanley, H. Tanaka, C. Vega, L. Xu, L. G. M. Pettersson, "Water: A Tale of Two Liquids", *Chem. Rev.* **116** (2016), no. 13, p. 7463-7500.
[68] K. H. Kim, K. Amann-Winkel, N. Giovambattista, A. Späh, F. Perakis, H. Pathak, M. L. Parada, C. Yang, D. Mariedahl, T. Eklund, T. J. Lane, S. You, S. Jeong, M. Weston, J. H. Lee, I. Eom, M. Kim, J. Park, S. H. Chun, P. H. Poole, A. Nilsson, "Experimental Observation of the Liquid-Liquid Transition in Bulk Supercooled Water under Pressure", *Science* **370** (2020), no. 6519, p. 978-982.
[69] M. A. Anisimov, M. Duška, F. Caupin, L. E. Amrhein, A. Rosenbaum, R. J. Sadus, "Thermodynamics of Fluid Polyamorphism", *Phys. Rev. X* **8** (2018), no. 1, article no. 011004.
[70] F. Caupin, M. A. Anisimov, "Minimal Microscopic Model for Liquid Polyamorphism and Waterlike Anomalies", *Phys. Rev. Lett.* **127** (2021), no. 18, article no. 185701.
[71] A. Zaragoza, C. S. P. Tripathi, M. A. Gonzalez, J. L. F. Abascal, F. Caupin, C. Valeriani, "Effect of Dissolved Salt on the Anomalies of Water at Negative Pressure", *J. Chem. Phys.* **152** (2020), no. 19, article no. 194501.
[72] L. C. Kah, T. W. Lyons, J. T. Chesley, "Geochemistry of a 1.2 Ga Carbonate-Evaporite Succession, Northern Baffin

and Bylot Islands: Implications for Mesoproterozoic Marine Evolution", *Precambrian Research* **111** (2001), no. 1-4, p. 203-234.

[73] S. M. Roberts, R. J. Spencer, "Paleotemperatures Preserved in Fluid Inclusions in Halite", *Geochim. Cosmochim. Acta* **59** (1995), no. 19, p. 3929-3942.

[74] T. K. Lowenstein, J. Li, C. B. Brown, "Paleotemperatures from fluid inclusions in halite: method verification and a 100,000 year paleotemperature record, Death Valley, CA", *Chem. Geol.* **150** (1998), no. 3–4, p. 223-245.

[75] E. Guillerm, V. Gardien, D. Ariztegui, F. Caupin, "Restoring Halite Fluid Inclusions as an Accurate Palaeothermometer: Brillouin Thermometry versus Microthermometry", *Geostand. Geoanal. Res.* **44** (2020), no. 2, p. 243-264.

[76] A. Fall, J. D. Rimstidt, R. J. Bodnar, "The Effect of Fluid Inclusion Size on Determination of Homogenization Temperature and Density of Liquid-Rich Aqueous Inclusions", *American Mineralogist* **94** (2009), no. 11-12, p. 1569-1579.

[77] D. Marti, Y. Krüger, D. Fleitmann, M. Frenz, J. Rička, "The Effect of Surface Tension on Liquid–Gas Equilibria in Isochoric Systems and Its Application to Fluid Inclusions", *Fluid Phase Equilib.* **314** (2012), p. 13-21.

[78] Y. Krüger, D. Marti, R. H. Staub, D. Fleitmann, M. Frenz, "Liquid–Vapour Homogenisation of Fluid Inclusions in Stalagmites: Evaluation of a New Thermometer for Palaeoclimate Research", *Chem. Geol.* **289** (2011), no. 1-2, p. 39-47.

[79] F. Caupin, "Effects of Compressibility and Wetting on the Liquid-Vapor Transition in a Confined Fluid", *J. Chem. Phys.* **157** (2022), no. 5, article no. 054506.

[80] Y. Krüger, P. Stoller, J. Rička, M. Frenz, "Femtosecond Lasers in Fluid-Inclusion Analysis: Overcoming Metastable Phase States", *Eur. J. Mineral.* **19** (2007), no. 5, p. 693-706.

[81] Y. Krüger, J. M. García-Ruiz, À. Canals, D. Marti, M. Frenz, A. E. S. Van Driessche, "Determining Gypsum Growth Temperatures Using Monophase Fluid Inclusions–Application to the Giant Gypsum Crystals of Naica, Mexico", *Geology* **41** (2013), no. 2, p. 119-122.

[82] M. E. Mekki-Azouzi, C. S. P. Tripathi, G. Pallares, V. Gardien, F. Caupin, "Brillouin Spectroscopy of Fluid Inclusions Proposed as a Paleothermometer for Subsurface Rocks", *Sci. Rep.* **5** (2015), no. 1, article no. 13168.

[83] E. Guillerm, V. Gardien, N. S. Brall, D. Ariztegui, M. J. Schwab, I. Neugebauer, N. D. Waldmann, A. Lach, F. Caupin, in preparation.

[84] I. Sirota, Y. Enzel, N. G. Lensky, "Temperature Seasonality Control on Modern Halite Layers in the Dead Sea: In Situ Observations", *GSA Bulletin* **129** (2017), no. 9-10, p. 1181-1194.

[85] N. S. Brall, V. Gardien, D. Ariztegui, P. Sorrel, E. Guillerm, F. Caupin, "Reconstructing Lake Bottom Water Temperatures and Their Seasonal Variability in the Dead Sea Basin during MIS5e", *Depositional Rec.* **8** (2022), no. 2, p. 616-627.